Atmos. Chem. Phys. Discuss., https://doi.org/10.5194/acp-2018-1200
Manuscript under review for journal Atmos. Chem. Phys.
Discussion started: 21 November 2018

Atmospheric Chemistry and Physics Discussions

Measuring Light Absorption by Organic Aerosols: Correction Factors for Solvent Extraction-Based Photometry Techniques

Nishit Shetty[1], Apoorva Pandey[1], Stephen Baker[2], Wei Min Hao[2], Rajan K. Chakrabarty[1,3]

[1]Center for Aerosol Science and Engineering, Department of Energy, Environmental and Chemical Engineering, Washington University in St. Louis, St. Louis, MO 63130, USA

[2]USDA Forest Service, Rocky Mountain Research Station, Fire Sciences Laboratory, Missoula, Montana, USA

[3]McDonnell Center for the Space Sciences, Washington University in St. Louis, St. Louis, MO 63130, USA

Correspondence to: Rajan K. Chakrabarty (chakrabarty@wustl.edu)

Abstract

Recent studies have shown that organic aerosol (OA) could have a non-trivial role in atmospheric light absorption at shorter visible wavelengths. Good estimates of OA absorption are therefore necessary to accurately calculate radiative forcing due to these aerosols in climate models. One of the common techniques used to measure OA light absorption is the solvent extraction technique from filter samples which involves the use of a spectrophotometer to measure bulk absorbance of the solvent-soluble organic fraction of particulate matter. Measured bulk absorbance is subsequently converted to particle-phase absorption coefficient using correction factors. The appropriate correction factors to use for performing this conversion under varying scenarios of organic carbon (OC) to total carbon (TC) mass ratios has been an unexplored area of research. The conventional view is to apply a correction factor of 2 for water-extracted OA based on Mie calculations.

Here, we performed a comprehensive laboratory study involving three solvents (water, methanol, and acetone) to investigate the corrections factors for converting from bulk-to-particle phase

Atmos. Chem. Phys. Discuss., https://doi.org/10.5194/acp-2018-1200
Manuscript under review for journal Atmos. Chem. Phys.
Discussion started: 21 November 2018

Atmospheric Chemistry and Physics Discussions

absorption coefficients ($b_{abs,OA}/b_{abs,bulk}$) for primary OA emitted from biomass burning. We parametrized these correction factors as a function of OC/TC mass ratio and single scattering albedo (SSA). We observed these correction factors to be a function of the OC/TC ratio of the aerosol, and that the conventionally used correction factor of 2 for water-extracted OA could severely underpredict OA absorption at high EC mass fractions. We recommend using $b_{abs,OA}/b_{abs,bulk}$ values between 2 and 11 for water extracts and values between 1 and 4 for methanol extracts based on OC/TC ratios, for EC mass fractions less than 0.25. Furthermore, a linear correlation between SSA and OC/TC ratio was also established. Finally, from the spectroscopic data, we analyzed the differences in Absorption Ångström Exponents (AÅE) obtained from bulk- and particulate-phase measurements. We noted that AÅE from bulk measurements deviate significantly from their OA counterparts.

1 Introduction

Carbonaceous aerosols constitute a major short-lived climate pollutant, and even though they have been studied extensively in recent years, estimates of their contribution to shortwave radiative forcing remains highly uncertain (IPCC, 2013). Based on their thermal-refractory properties, carbonaceous aerosols are categorized as elemental carbon (EC) or organic carbon (OC) (Chow et al., 2007b; Bond et al., 2013), and the sum of OC and EC is referred to as total carbon (TC). When defined optically, the refractory EC component is approximately referred to as black carbon (BC) (Chow et al. 2007b; Bond et al., 2013); BC aerosol constitute the strongest of the light absorbing aerosol components in the atmosphere (Andreae and Gelencsér 2006; Ramanathan and Carmichael 2008; IPCC, 2013). While BC absorbs strongly in the visible spectrum, the contribution of OC towards absorption has largely been neglected, even though many studies have demonstrated significant OC absorption at lower visible wavelengths (Yang et

al., 2009; Chen and Bond, 2010; Chakrabarty et al., 2010; Chen et al., 2018). The atmospheric mass of OC can be 3-12 times larger than that of BC (Husain et al., 2007; Zhang et al., 2008) which warrants its inclusion as an atmospheric light absorber. Only recently have a few global modeling studies incorporated radiative forcing by organic aerosol (OA) absorption (Chung et al., 2012; Feng et al., 2013; Lin et al., 2014). Thus, having accurate estimates for OA absorption is necessary to help improve climate models.

A convenient and prevalent methodology of measuring OA absorption is based on collecting aerosol particles on a filter substrate followed by extracting the organic compounds into a solvent. This is a good analytical method used in many studies as it excludes any interference from EC and provides only the OC absorption spectra (Mo et al., 2017; Chen and Bond, 2010; Liu et al., 2013). The absorbance of the organic chromophores in the solvent extract is measured using an ultraviolet-visible (UV-Vis) spectrophotometer and the imaginary part of the complex refractive index of the solvent is calculated using the measured absorbance and extract concentrations. The absorbance values can be converted to corresponding bulk phase absorption coefficients ($b_{abs,bulk}$), and the imaginary index along with an assumed number size distribution can be used as inputs to Mie theory for calculating the absorption coefficient for the dissolved OC particles. Past studies have suggested that $b_{abs,bulk}$ is not representative of the corresponding particulate-phase organic aerosol absorption coefficient ($b_{abs,OA}$) (Liu et al., 2013; Moosmüller et al., 2011). The situation thus warrants appropriate correction factors be applied to account for the size-dependent absorption properties of OA when estimating $b_{abs,OA}$ using the solvent-extract methodology. Using absorption coefficients determined with Mie Theory, previous studies have determined a narrow range of solvent-dependent correction factors from 2 for water extracts to 1.8 for methanol extracts, all corresponding to a mean particle diameter of 0.5 μm (Liu et al.,

2013; Liu et al., 2016; Liu et al., 2014; Washenfelder et al., 2015). These correction factors have been deemed relatively independent of particle size as long as the diameters do not get much smaller than the wavelength of light, in which case their values fall to a range of 0.69 - 0.75 (Sun et al., 2007). Further, these factors were calculated assuming homogeneous composition and external mixing states of the OC aerosol in addition to fixed values of the real part of the refractive index and effective density. No attempts have been made to quantify the variation in these correction factors with varying aerosol intrinsic properties, such as the single scattering albedo, and EC/OC ratios, even though these properties influence the types and fractions of organics extracted by a given solvent (Zhang et al., 2013; Saleh at al., 2014) thereby affecting $b_{abs,bulk}$.

In-situ measurement of particulate-phase absorption coefficient is commonly and accurately accomplished using a photoacoustic spectrometer (PAS) (Lack et al., 2006; Arnott et al., 2005; Arnott et al., 2003). However, a single-wavelength PAS cannot distinguish between absorption by OC and BC aerosol and it typically measures the total particle-phase absorption coefficient ($b_{abs,tot}$) of the aerosol population in the cell (Moosmüller et al., 2009). One must make use of a multi-wavelength PAS using which $b_{abs,OA}$ could be separated out from that of BC, based on the difference in their Absorption Ångström Exponent (AÅE) (Washenfelder et al., 2015; Arola et al., 2011; Kirchstetter and Thatcher; 2012). The AÅE for pure BC is well-constrained at 1 in the visible and near-infrared wavelengths (Moosmüller et al., 2009). The value of $b_{abs,OA}$ is then the difference between $b_{abs,tot}$ and the BC absorption coefficient. A correction factor ($b_{abs,OA}/b_{abs,bulk}$) can thus be determined, provided simultaneous measurements of bulk- and particle-phase absorption properties have been carried out during a study.

93 Here, we burnt a range of different biomass fuels under different combustion conditions and the
94 resulting aerosol emissions were passed through various in-situ instruments while simultaneously
95 being collected on quartz-fiber filters. The particle phase absorption coefficient was obtained
96 using integrated photoacoustic-nephelometer spectrometers (IPNs) at wavelengths 375, 405 and
97 1047 nm. Organics collected on quartz-fiber filters were extracted in water, acetone, and
98 methanol, and corresponding $b_{abs,bulk}$ values were calculated. These values were compared with
99 corresponding $b_{abs,OA}$, and the change in $b_{abs,OA}/b_{abs,bulk}$ with varying single scattering albedo
100 (SSA) values and OC/TC ratios was established. SSA was parametrized with the OC/TC ratios
101 with trends similar to those observed by Pokhrel et al., (2016). AÅE from spectroscopic data for
102 bulk and particle phase measurements were compared, and the Mie Theory based correction
103 factor was also verified for a few samples.

104 **2 Methods:**

105 **2.1 Sample generation and collection**

106 Fig. 1 is a schematic diagram of our experimental setup, which consists of a sealed 21 m^3
107 stainless-steel combustion chamber housing a fan for mixing and recirculation (Sumlin et al.,
108 2018b). Aerosol samples were generated by burning several types of biomass including pine, fir,
109 grass, sage, and cattle dung (sources are given in the Supplementary Information). During a
110 chamber burn, 10-50 g of a given biomass was placed in a stainless-steel pan and ignited by a
111 butane lighter. The chamber exhaust was kept closed for the duration of a given experiment. The
112 biomass bed was either allowed to burn to completion or it was prematurely extinguished and
113 brought to a smoldering phase by extinguishing the flame beneath a lid. The different
114 combustion conditions were used to generate samples with varying properties: OC/TC ratios

ranged from 0.55-1, and SSA values ranged from 0.56-0.98 for wavelengths of 375, 405, and 1047 nm.

For one set of experiments, the particles were directly sampled from the chamber; in another set, the sampling was done from a hood placed over the burning biomass. A diffusion dryer removed excess water from the sample stream, and the gas-phase organics were removed by a pair of activated parallel-plate semi-volatile organic carbon (SVOC) denuders. The gas-phase organics were stripped to reduce artifacts produced by the adsorption of organic vapors on the quartz filters. The aerosols were finally sent to a 208-liter stainless-steel barrel, from which they were continuously sampled by the three IPNs and a scanning mobility particle sizer (SMPS, TSI, Inc.). The SMPS was not used in all the experiments, however, it gave an estimate of the range over which the size distributions varied and was used to determine the geometric mean of the size distribution. The real-time absorption and scattering coefficients were measured by the IPNs, and samples were simultaneously collected on quartz fiber filters once a steady state signal was achieved. The absorption and scattering coefficients were used to calculate the SSA, which is simply the scattering coefficient divided by the extinction coefficient. Radiative forcing calculations for absorbing OC require good estimates of OC absorption at different SSA values (Lin et al, 2014; Feng et al, 2013; Chakrabarty et al, 2010) underscoring the need for correction factors as a function of SSA. The particles were passed through the filter samplers at a flowrate of 5 $lmin^{-1}$, with sampling times ranging from 2-15 minutes. Two or more filters were collected for each steady state condition. One of these filters was used to determine the OC and EC fractions of the deposited particles, and the other filters were used for the extraction experiments.

2.2 Analytical Techniques

2.2.1 Absorption by solvent extracted OC

Quartz filters (Pallflex Tissuquartz) collected during sampling were split into four quarters, and each quarter was extracted using either deionized water, acetone, hexane, or methanol. The absorption by hexane extracts were low and prone to errors, so data for its extracts were not analyzed. The filters were placed in a covered beaker along with 3-5 ml of the solvent for 24 hours. The solvent volumes were measured both before and after the extraction and the differences between the two measurements were within 8%. The extracts were then passed through syringe filters with 0.22 μm pores to remove any impurities introduced by the extraction process.

The light absorbance of the extracts was measured using a UV-Vis spectrophotometer (Varian Inc., Cary 50) at wavelengths from 300 nm to 800 nm. To compare the absorbance (A(λ)) of the chromophores in the solution with the absorption coefficient of the particles in the atmosphere, all absorbance values were converted to solution-phase absorption coefficients at given wavelengths ($b_{abs,bulk}(\lambda)$):

$$b_{abs,bulk}(\lambda) = (A(\lambda) - A(700))\frac{V_l}{V_a * l} \cdot \ln(10), \quad (1)$$

where V_l is the volume of solvent the filter was extracted into, V_a is the volume of air that passed over the given filter area, and l is the optical path length that the beam traveled through the cuvette (1 cm). The absorbance at a given wavelength is normalized to the absorbance at 700 nm to account for any signal drift within the instrument. The resulting absorption coefficient (m^{-1}) was multiplied by ln(10) to convert from base 10 (provided by the UV-Vis spectrophotometer) to natural logarithms.

2.2.2 Absorption by BC and OC in particle phase

Atmos. Chem. Phys. Discuss., https://doi.org/10.5194/acp-2018-1200
Manuscript under review for journal Atmos. Chem. Phys.
Discussion started: 21 November 2018

Atmospheric Chemistry and Physics Discussions

To estimate the BC absorption at 375 nm and 405 nm, the absorption data from the IPN operated in the infrared regime at a wavelength of 1047 nm was converted to equivalent particulate absorption at the near UV wavelengths, using a BC absorption Ångström exponent ($AÅE_{BC}$) value of 1 (Kirchstetter et al., 2004; Andreae and Gelencsér, 2006). The assumption here being that all the absorption at 1047 nm could be attributed to BC aerosol (Bahadur et al., 2012). The BC light absorption coefficient at shorter wavelengths ($b_{abs,BC}(\lambda_1)$) was calculated by:

$$b_{abs,BC}(\lambda_1) = b_{abs,IPN}(1047).\left(\frac{\lambda_1}{1047}\right)^{-AÅE_{BC}}, \quad (2)$$

where λ_1 is the wavelength at which the absorption will be calculated and AÅE is defined for a pair of wavelengths λ_1 and λ_2 as the exponent in a power law expressing the ratio of the absorption coefficients as follows (Moosmüller et al., 2009):

$$AÅE(\lambda_1\lambda_2) = \frac{ln\left[{b_{abs}(\lambda_1)}/{b_{abs}(\lambda_2)}\right]}{ln\left[{\lambda_2}/{\lambda_1}\right]}, \quad (3)$$

AÅE is an optical descriptor of the inherent material property. For BC particles, typical values of AÅE ≈1, while for OC particles AÅE > 4 (Moosmüller et al., 2009). The value of $b_{abs,BC}$ at 375nm and 405nm was then subtracted from $b_{abs,tot}$ at those wavelengths to calculate $b_{abs,OA}$. The ratio $b_{abs,OA}(\lambda)/b_{abs,bulk}(\lambda)$ was calculated to give the conversion factor for converting from the bulk solvent phase absorption to OA absorption coefficient.

The organic and elemental carbon compositions of the filters were measured with a thermal-optical OC/EC analyzer (Sunset Laboratory, Tigard, OR) using the Interagency Monitoring of Protected Visual Environments (IMPROVE)-A analysis method (Chow et al., 2007a). The

178 OC/TC ratios were assumed to be constant for a given steady state IPN reading, which allowed
179 us to relate the absorption data to the OC/TC data.

180 **2.3 Mie Theory Calculations**

181 A commonly used method to correct for differences between the chromophore absorption in
182 solution and aerosol particle absorption is by using Mie Theory (Liu et al., 2013; Washenfelder
183 et al., 2015). The imaginary part (k) of the complex refractive index $m = n + ik$ can be
184 determined from the bulk solution absorption data and converted to an equivalent organic carbon
185 particulate absorption, using Mie Theory along with a range of assumptions.

186 To find k, the mass absorption efficiency (α/ρ) was determined using the absorbance data and the
187 OC mass concentration in the solution:

188 $$\frac{\alpha(\lambda)}{\rho} = \frac{b_{abs,bulk}(\lambda)}{M}, \quad (4)$$

189 where $b_{abs,bulk}(\lambda)$ is the bulk absorption coefficient determined in Eq. (1), and M is the mass
190 concentration of OC in the solution. In the given study, the mass concentration was measured for
191 some of the water extracts using a total organic carbon (TOC) analyzer (Shimadzu, TOC-L). The
192 corresponding water-soluble organic carbon (WSOC) was then used to estimate α/ρ of the bulk
193 solution. The calculated α/ρ was then used to determine k for the WSOC by:

194 $$k(\lambda) = \frac{\rho.\lambda.\left(\frac{\alpha(\lambda)}{\rho}\right)}{4\pi}, \quad (5)$$

195 where λ is the light wavelength at which k needs to be calculated, and ρ is the density of the
196 dissolved organic compounds. A ρ value of 1.6 (Alexander et al., 2008) was used to calculate the
197 k values, and also used in all subsequent calculations using density. A Mie based inversion

algorithm was used to extract the real part of the refractive index (*n*) using data from the SMPS and IPN (Sumlin et al., 2018a). A sensitivity analysis was performed by varying the n value from 1.4 to 2, and the change in Mie calculated absorption was within 18%. The size distribution for the WSOC was estimated assuming the same geometric mean and standard deviation as that of the original aerosol, but with number concentrations calculated based on the extracted mass. Calculations for the number concentration are provided in the SI.

After the size distribution and complex refractive index were determined, they were used to calculate the absorption coefficient based on Mie Theory, which was then compared to $b_{abs,bulk}$ to determine Mie based correction factors for converting from bulk to particle phase absorption.

3 Results and discussion

3.1 Correction factor as a function of Single Scattering Albedo

Fig. 2 shows the trends in $b_{abs,OA}(\lambda)/b_{abs,bulk}(\lambda)$ with varying SSA. The error bars account for uncertainties in IPN measurements, UV-Vis spectrophotometer measurements, flowrates for filter sampling, and extract volume measurements. The SSA values of fractal BC aggregates are between 0.3-0.4 for light wavelengths of 400 nm (Cheng et al., 2013), and due to this particularly low SSA of BC compared to OC, an increase in the BC content of the aerosol composition is expected with decreasing SSA. This relation is explored further in Section 3.2 and 3.3. Fig 2. also indicates that the light absorbed by methanol and acetone extracts were almost identical and would imply that the amount and type of OC extracted by the two solvents were similar, as seen in other studies as well (Chen and Bond, 2010; Wang et al., 2014). The differences between the conversion factors for water and methanol are discussed further in Section 3.3. The differences

between the mean values of $b_{abs,OA}(\lambda)/b_{abs,bulk}(\lambda)$ at 375 and 405 nm were less than or close to the errors associated with them, hence any trends with wavelength were not explored.

The value of $b_{abs,OA}(\lambda)/b_{abs,bulk}(\lambda)$ approached a constant in the measured range of data. A power law ($y = k_0 + k_1 x^{k_2}$) was used to fit the points in Fig. 2, and the corresponding fit parameters, along with root mean square error (RMSE) values, are listed in Table 1. The value of BC AÅE has a significant effect on the conversion factor for particles with SSA smaller than 0.7 at 375 nm and smaller than 0.825 at 405 nm. A sensitivity analysis was performed to observe the change in $b_{abs,OA}(\lambda)/b_{abs,bulk}(\lambda)$ due to a change in BC AÅE from 0.85 to 1.1, which are typical values observed in other studies (Lack et al., 2008; Bergstrom et al., 2007; Lan et al., 2013). For the correction factors at 375 nm, on varying the AÅE we calculated a change of less than 14% for aerosols with SSA greater than 0.7, whereas a change as high as 200% was seen for particles with SSA less than 0.7. Similar changes in the correction factor were observed for SSA less than 0.825 at 405 nm. These fluctuations indicate that the current method is best suited for particles with relatively higher SSA values. The perforated lines in Fig. 2 separate points with high AÅE based fluctuations (at lower SSA values) from those that have relatively small variation with changes in the BC AÅE.

3.2 SSA parametrized with OC/TC

Fig. 3 shows the variation in SSA with change in the OC/TC ratio of the aerosol. The OC/TC ratio was determined using the IMPROVE-A TOR protocol with the thermal optical EC/OC analyzer at Sunset laboratories. The resulting fits for the plots in Fig. 3 are linear with correlation coefficients of 0.9 and 0.95 for wavelengths 375 nm and 405 nm respectively. A linear relation between the SSA and the EC/TC ratio (which is simply the OC/TC ratio subtracted from 1) was also observed by Pokhrel et al. (2016). However, when the data from that study were converted

to OC/TC values for comparison, it was noted that the slopes and intercepts of the resulting fits were different from those observed in this study. Table 2 has a list of the slope and intercept of fits for comparable wavelengths in both studies, along with the correlation coefficient.

In Fig. 3, the points corresponding to high OC/TC ratios are associated with SSA values that are close to 1, because pure OC aerosols are predominantly light-scattering. However, it is also noted that the aerosols with OC/TC of 1 have SSA values less than 1 at the measured wavelengths and the fit values indicate that the absorption has large spectral variation. The fit yielded SSA values of 0.86 and 0.95 at 375 and 405 nm respectively indicating that the aerosols can be categorized as brown carbon (Chakrabarty et al. 2010). Thus, it is useful to note that the fit parameters in Table 2 capture the effects of the brown carbon, because the SSA values for pure OC are below 1 at both wavelengths.

A useful conclusion from Fig. 3 is that the OC/TC ratio can predict the SSA of the aerosol even though information on size distributions, burn conditions, and fuel type are not used. This correlation, however, has high variations at OC/TC ratios very close to 1, where fuel type and burn conditions do dictate the composition and absorption properties (Chen and Bond, 2010; Budisulistiorini et al., 2017) of organics released and hence a larger range of SSA values exist for the given OC/TC value. Further studies need to be conducted using more fuels with a variety of distinct size distributions and burn conditions to determine the validity and exact parameters for the fit.

3.3 Correction factor as a function of OC/TC ratio

Fig. 4 depicts the variation in $b_{abs,OA}(\lambda)/b_{abs,bulk}(\lambda)$ with different OC/TC ratios. Because the OC/TC ratio and the SSA are well correlated, we expect to see a similar trend for Fig. 4 as in

Fig. 2. The correction factor for the three solvents approaches a constant as the OC/TC ratio decreases. However, it is important to note that the magnitude of the conversion factor could change due to uncertainties in the value of the AÅE used for the BC. A power law like the one in Fig. 2 was fit to the data in Fig. 4. The fit parameters for the different solvents at the two wavelengths, along with the RMSE value for each fit, are presented in Table 3. The errors due to uncertainty in BC AÅE are more pronounced at higher EC fractions, leading to high fluctuations in correction factors at OC/TC ratios below 0.75. Thus, the correction factors determined by this method are valid primarily for aerosols with EC fraction < 0.25.

We also fit an exponential curve to $b_{abs,OA}(\lambda)/b_{abs,bulk}(\lambda)$ as a function of EC/OC values ($y = k_0 + k_1*(1-\exp(-(EC/OC)/k_2))$). The fits had comparable RMSE values, but because strong relationships between the SSA and OC/TC ratios were previously established, the plots described here continue along those lines. The curves plotted with EC/OC, along with the parameters for the fits, are provided in the SI.

The differences in the magnitudes of the correction factors between acetone/methanol extracts and water extracts increase as the EC composition of the aerosols increases. A change in the absorption properties of OC at different EC/OC ratios was observed by Saleh et al. (2014) which could explain the increasing difference in the magnitude of $b_{abs,OA}/b_{abs,bulk}$ between water and methanol/acetone extracts. The increasing difference in absorbance between water and methanol with increasing EC content would indicate a decrease in the total absorbing WSOC compared to total absorbing OC. An increase in the amount of water insoluble organic carbon with increasing EC content of the aerosol was also observed by Zhang et al. (2013), which strengthens our hypothesis for a steeper increase in $b_{abs,OA}(\lambda)/b_{abs,bulk}(\lambda)$ of water extracts as compared to methanol with increasing BC mass fraction of the aerosol.

Atmos. Chem. Phys. Discuss., https://doi.org/10.5194/acp-2018-1200
Manuscript under review for journal Atmos. Chem. Phys.
Discussion started: 21 November 2018

3.4 Variations in AÅE with solvents and OC/TC ratios

The AÅE values, for organics extracted in different solvents and those obtained from $b_{abs,OA}$ are compared in Table 4. The AÅE values were calculated between λ = 375 and 405 nm from spectrophotometer data. Consistent with previous studies (Chen and Bond, 2010; Zhang et al., 2013; Liu et al., 2013), the AÅE values of the water extracts were larger than the AÅE of the acetone and methanol extracts. The lower AÅE values for the methanol and acetone extracts compared to water would indicate that the former two solvents are better at extracting the higher molecular weight compounds than water, and they can thus absorb more light at longer wavelengths, leading to smaller AÅE.

The AÅE values calculated for OA ranged from 4.4 to 14.61 and overall the AÅE for OA measurements decreased with increasing EC mass fraction in the aerosol. The AÅE calculated for OC in both the particle- and bulk-phase decreased at lower OC/TC ratios indicating a drastic decrease in the spectral dependence of OC co-emitted with BC. Table 4 shows that AÅE values for OA were greater than or close to their bulk counterparts at OC/TC ratios close to 1. These bulk measurements of AÅE suggest that they deviate significantly from the spectral dependence of OC in the particle phase, and future studies and models should not use AÅE data from bulk measurements to be representative of the particle phase.

3.4 Mie Calculations

The absorption coefficient determined from the bulk absorbance using Eq. (1) was compared to the absorption coefficient calculated using Mie theory for three samples of smoldering sage. The EC/OC analysis (IMPROVE-A protocol) determined that these samples consisted purely of OC,

and because the SMPS measurements and TOC analysis were not performed on all samples, the three samples of sage were considered optimum for the Mie calculations.

The Mie based correction factors for bulk to particulate absorption for the three samples are presented in Table 5. The calculated correction factors at 375 nm and 405 nm are close to 2 as observed in previous studies (Liu et al., 2013; Washenfelder et al., 2015). The values for the correction factor vary from 1.99 to 2.05 at 375 nm and 2.15 to 2.29 at 405 nm. However, it is important to note that the correction factor of 2 cannot be used for all conditions, as observations from Fig. 2 and Fig. 4 indicate that the Mie theory based correction factor might severely underestimate the absorption by the total absorbing OA particles in accumulation mode.

4 Conclusions

Under controlled laboratory conditions, we determined the factor required for converting the absorption coefficient of bulk solvent extracts to particle phase absorption coefficients for organic aerosol emissions from biomass combustion. We combusted a range of different wildland fuels under different combustion conditions, generating a span of different SSA and OC/TC values. The SSA values ranged from 0.55 to 0.87 at 375 nm, and from 0.69 to 0.95 at 405 nm, the OC/TC values ranged from 0.55 to 1. We observed that the conversion factor tends towards a constant with increasing EC content for the range of SSA and OC/TC analyzed, and these factors were parametrized with the SSA and OC/TC of the total aerosol for three solvents (water, methanol, and acetone). We also demonstrated that the SSA and OC/TC ratios can be well parametrized with a linear fit that captures the effects of brown carbon aerosol. We analyzed the validity of the conventionally used correction factor of 2 for water extracts of aerosol particles in accumulation mode and noted that, while the factor is reproducible, its use can significantly underestimate OA absorption. We recommend using $b_{abs,OA}/b_{abs,bulk}$ values between

2 and 11 for water extracts and values between 1 and 4 for methanol extracts based on OC/TC ratios for EC mass fractions less than 0.25.

For future studies, a better technique to quantify BC absorption at lower wavelengths, such as a thermodenuder to strip off all OC, or a single particle soot photometer along with core-shell Mie calculations to determine BC absorption can be used to decrease uncertainties from BC AÅE. Here, BC is assumed to be externally mixed with OC; correction factors accounting for BC absorption enhancement can be explored to improve estimates of $b_{abs,OA}/b_{abs,bulk}$. Zhang et al. (2013) observed lower AÅE for WSOC from a particle into liquid sampler (PILS) than for methanol extracts. The hypothesis was that the highly dilute environment in PILS increased dissolution of organics in water. The validity and reason for lower AÅE from PILS data can be explored in future studies along with finding corresponding differences in $b_{abs,OA}/b_{abs,bulk}$.

Author Contributions

RKC conceived of this study and designed the experiments. SB and WMH collected the fuels for the experiments and performed EC/OC analysis on the sampled filters. NS and AP carried out the experiments and analysed the data. NS prepared the manuscript with input from all co-authors.

Acknowledgements

This work was partially supported by the National Science Foundation under Grant No. AGS1455215, NASA ROSES under Grant No. NNX15AI66G.

References

Alexander, D. T., Crozier, P. A., and Anderson, J. R.: Brown carbon spheres in East Asian outflow and their optical properties, Science, 321, 833-836, 2008.

Andreae, M., and Gelencsér, A.: Black carbon or brown carbon? The nature of light-absorbing carbonaceous aerosols, Atmospheric Chemistry and Physics, 6, 3131-3148, 2006.

Arnott, W., Moosmüller, H., Sheridan, P., Ogren, J., Raspet, R., Slaton, W., Hand, J., Kreidenweis, S., and Collett Jr, J.: Photoacoustic and filter-based ambient aerosol light absorption measurements: Instrument comparisons and the role of relative humidity, Journal of Geophysical Research: Atmospheres, 108, AAC 15-11-AAC 15-11, 2003.

Arnott, W. P., Hamasha, K., Moosmüller, H., Sheridan, P. J., and Ogren, J. A.: Towards aerosol light-absorption measurements with a 7-wavelength aethalometer: Evaluation with a photoacoustic instrument and 3-wavelength nephelometer, Aerosol Science and Technology, 39, 17-29, 2005.

Arola, A., Schuster, G., Myhre, G., Kazadzis, S., Dey, S., and Tripathi, S.: Inferring absorbing organic carbon content from AERONET data, Atmospheric Chemistry and Physics, 11, 215-225, 2011.

Bahadur, R., Praveen, P. S., Xu, Y., and Ramanathan, V.: Solar absorption by elemental and brown carbon determined from spectral observations, Proceedings of the National Academy of Sciences, 201205910, 2012.

Bergstrom, R. W., Pilewskie, P., Russell, P. B., Redemann, J., Bond, T. C., Quinn, P. K., and Sierau, B.: Spectral absorption properties of atmospheric aerosols, Atmospheric Chemistry and Physics, 7, 5937-5943, 2007.

Bond, T. C., Doherty, S. J., Fahey, D., Forster, P., Berntsen, T., DeAngelo, B., Flanner, M., Ghan, S., Kärcher, B., and Koch, D.: Bounding the role of black carbon in the climate system: A scientific assessment, Journal of Geophysical Research: Atmospheres, 118, 5380-5552, 2013.

Budisulistiorini, S. H., Riva, M., Williams, M., Chen, J., Itoh, M., Surratt, J. D., and Kuwata, M.: Light-absorbing brown carbon aerosol constituents from combustion of Indonesian peat and biomass, Environmental Science & Technology, 51, 4415-4423, 2017.

Chakrabarty, R., Moosmüller, H., Chen, L.-W., Lewis, K., Arnott, W., Mazzoleni, C., Dubey, M., Wold, C., Hao, W., and Kreidenweis, S.: Brown carbon in tar balls from smoldering biomass combustion, Atmospheric Chemistry and Physics, 10, 6363-6370, 2010.

Chen, Y., and Bond, T.: Light absorption by organic carbon from wood combustion, Atmospheric Chemistry and Physics, 10, 1773-1787, 2010.

Chen, Y., Wang, H., Singh, B., Ma, P. L., Rasch, P. J., and Bond, T. C.: Investigating the linear dependence of direct and indirect radiative forcing on emission of carbonaceous aerosols in a global climate model, Journal of Geophysical Research: Atmospheres, 123, 1657-1672, 2018.

Cheng, T., Gu, X., Wu, Y., Chen, H., and Yu, T.: The optical properties of absorbing aerosols with fractal soot aggregates: Implications for aerosol remote sensing, Journal of Quantitative Spectroscopy and Radiative Transfer, 125, 93-104, 2013.

Chow, J. C., Watson, J. G., Chen, L.-W. A., Chang, M. O., Robinson, N. F., Trimble, D., and Kohl, S.: The IMPROVE_A temperature protocol for thermal/optical carbon analysis: maintaining consistency with a long-term database, Journal of the Air & Waste Management Association, 57, 1014-1023, 2007a.

Chow, J. C., Yu, J. Z., Watson, J. G., Hang Ho, S. S., Bohannan, T. L., Hays, M. D., and Fung, K. K.: The application of thermal methods for determining chemical composition of carbonaceous aerosols: A review, Journal of Environmental Science and Health Part A, 42, 1521-1541, 2007b.

Chung, C. E., Ramanathan, V., and Decremer, D.: Observationally constrained estimates of carbonaceous aerosol radiative forcing, Proceedings of the National Academy of Sciences, 109, 11624-11629, 2012.

Feng, Y., Ramanathan, V., and Kotamarthi, V.: Brown carbon: a significant atmospheric absorber of solar radiation?, Atmospheric Chemistry and Physics, 13, 8607-8621, 2013.

Husain, L., Dutkiewicz, V. A., Khan, A., and Ghauri, B. M.: Characterization of carbonaceous aerosols in urban air, Atmospheric Environment, 41, 6872-6883, 2007.

IPCC: Climate Change: The Physical Science Basis, Contribution of Working Group I to the UN IPCC's 5th Assessment Report, Cambridge University Press, New York, USA, 2013.

Kirchstetter, T. W., Novakov, T., and Hobbs, P. V.: Evidence that the spectral dependence of light absorption by aerosols is affected by organic carbon, Journal of Geophysical Research: Atmospheres, 109, 2004.

Kirchstetter, T., and Thatcher, T.: Contribution of organic carbon to wood smoke particulate matter absorption of solar radiation, Atmospheric Chemistry and Physics, 12, 6067-6072, 2012.

Lack, D. A., Lovejoy, E. R., Baynard, T., Pettersson, A., and Ravishankara, A.: Aerosol absorption measurement using photoacoustic spectroscopy: Sensitivity, calibration, and uncertainty developments, Aerosol Science and Technology, 40, 697-708, 2006.

Lack, D. A., Cappa, C. D., Covert, D. S., Baynard, T., Massoli, P., Sierau, B., Bates, T. S., Quinn, P. K., Lovejoy, E. R., and Ravishankara, A.: Bias in filter-based aerosol light absorption measurements due to organic aerosol loading: Evidence from ambient measurements, Aerosol Science and Technology, 42, 1033-1041, 2008.

Lan, Z.-J., Huang, X.-F., Yu, K.-Y., Sun, T.-L., Zeng, L.-W., and Hu, M.: Light absorption of black carbon aerosol and its enhancement by mixing state in an urban atmosphere in South China, Atmospheric environment, 69, 118-123, 2013.

Lin, G., Penner, J. E., Flanner, M. G., Sillman, S., Xu, L., and Zhou, C.: Radiative forcing of organic aerosol in the atmosphere and on snow: Effects of SOA and brown carbon, Journal of Geophysical Research: Atmospheres, 119, 7453-7476, 2014.

Liu, J., Bergin, M., Guo, H., King, L., Kotra, N., Edgerton, E., and Weber, R.: Size-resolved measurements of brown carbon in water and methanol extracts and estimates of their contribution to ambient fine-particle light absorption, Atmospheric Chemistry and Physics, 13, 12389-12404, 2013.

Liu, J., Scheuer, E., Dibb, J., Ziemba, L. D., Thornhill, K. L., Anderson, B. E., Wisthaler, A., Mikoviny, T., Devi, J. J., and Bergin, M.: Brown carbon in the continental troposphere, Geophysical Research Letters, 41, 2191-2195, 2014.

Liu, X., Zhang, Y., Huey, L., Yokelson, R., Wang, Y., Jimenez, J., Campuzano-Jost, P., Beyersdorf, A., Blake, D., and Choi, Y.: Agricultural fires in the southeastern US during SEAC4RS: Emissions of trace gases and particles and evolution of ozone, reactive nitrogen, and organic aerosol, Journal of Geophysical Research: Atmospheres, 121, 7383-7414, 2016.

Mo, Y., Li, J., Liu, J., Zhong, G., Cheng, Z., Tian, C., Chen, Y., and Zhang, G.: The influence of solvent and pH on determination of the light absorption properties of water-soluble brown carbon, Atmospheric environment, 161, 90-98, 2017.

Moosmüller, H., Chakrabarty, R., and Arnott, W.: Aerosol light absorption and its measurement: A review, Journal of Quantitative Spectroscopy and Radiative Transfer, 110, 844-878, 2009.

Moosmüller, H., Chakrabarty, R., Ehlers, K., and Arnott, W.: Absorption Ångström coefficient, brown carbon, and aerosols: basic concepts, bulk matter, and spherical particles, Atmospheric Chemistry and Physics, 11, 1217-1225, 2011.

Pokhrel, R. P., Wagner, N. L., Langridge, J. M., Lack, D. A., Jayarathne, T., Stone, E. A., Stockwell, C. E., Yokelson, R. J., and Murphy, S. M.: Parameterization of single-scattering albedo (SSA) and absorption Ångström exponent (AAE) with EC/OC for aerosol emissions from biomass burning, Atmospheric Chemistry and Physics, 16, 9549-9561, 2016.

Ramanathan, V., and Carmichael, G.: Global and regional climate changes due to black carbon, Nature geoscience, 1, 221, 2008.

Saleh, R., Robinson, E. S., Tkacik, D. S., Ahern, A. T., Liu, S., Aiken, A. C., Sullivan, R. C., Presto, A. A., Dubey, M. K., and Yokelson, R. J.: Brownness of organics in aerosols from biomass burning linked to their black carbon content, Nature Geoscience, 7, 647, 2014.

452 Sumlin, B. J., Heinson, W. R., and Chakrabarty, R. K.: Retrieving the aerosol complex refractive
453 index using PyMieScatt: A Mie computational package with visualization capabilities, Journal of
454 Quantitative Spectroscopy and Radiative Transfer, 205, 127-134, 2018a.

455 Sumlin, B. J., Heinson, Y. W., Shetty, N., Pandey, A., Pattison, R. S., Baker, S., Hao, W. M., and
456 Chakrabarty, R. K.: UV–Vis–IR spectral complex refractive indices and optical properties of
457 brown carbon aerosol from biomass burning, Journal of Quantitative Spectroscopy and Radiative
458 Transfer, 206, 392-398, 2018b.

459 Sun, H., Biedermann, L., and Bond, T. C.: Color of brown carbon: A model for ultraviolet and
460 visible light absorption by organic carbon aerosol, Geophysical Research Letters, 34, 2007.

461 Wang, X., Heald, C., Ridley, D., Schwarz, J., Spackman, J., Perring, A., Coe, H., Liu, D., and
462 Clarke, A.: Exploiting simultaneous observational constraints on mass and absorption to estimate
463 the global direct radiative forcing of black carbon and brown carbon, Atmospheric Chemistry
464 and Physics, 14, 10989-11010, 2014.

465 Washenfelder, R., Attwood, A., Brock, C., Guo, H., Xu, L., Weber, R., Ng, N., Allen, H., Ayres,
466 B., and Baumann, K.: Biomass burning dominates brown carbon absorption in the rural
467 southeastern United States, Geophysical Research Letters, 42, 653-664, 2015.

468 Yang, M., Howell, S., Zhuang, J., and Huebert, B.: Attribution of aerosol light absorption to
469 black carbon, brown carbon, and dust in China–interpretations of atmospheric measurements
470 during EAST-AIRE, Atmospheric Chemistry and Physics, 9, 2035-2050, 2009.

471 Zhang, X., Wang, Y., Zhang, X., Guo, W., and Gong, S.: Carbonaceous aerosol composition
472 over various regions of China during 2006, Journal of Geophysical Research: Atmospheres, 113,
473 2008.

474 Zhang, X., Lin, Y.-H., Surratt, J. D., and Weber, R. J.: Sources, composition and absorption
475 Ångstrom exponent of light-absorbing organic components in aerosol extracts from the Los
476 Angeles Basin, Environmental science & technology, 47, 3685-3693, 2013.

477 **Figures and Tables:**

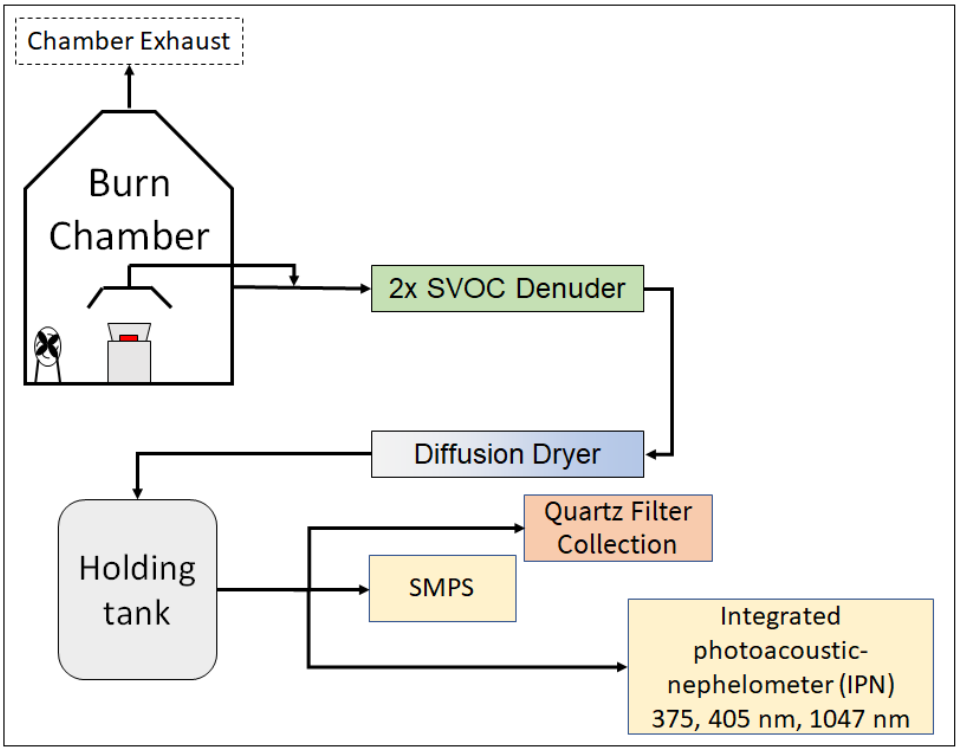

478

479 **Fig. 1:** A schematic representing the experimental setup. The aerosol emissions were either
480 sampled directly from the chamber wall or through a hood placed directly above the combusting
481 biomass.

482

Atmos. Chem. Phys. Discuss., https://doi.org/10.5194/acp-2018-1200
Manuscript under review for journal Atmos. Chem. Phys.
Discussion started: 21 November 2018

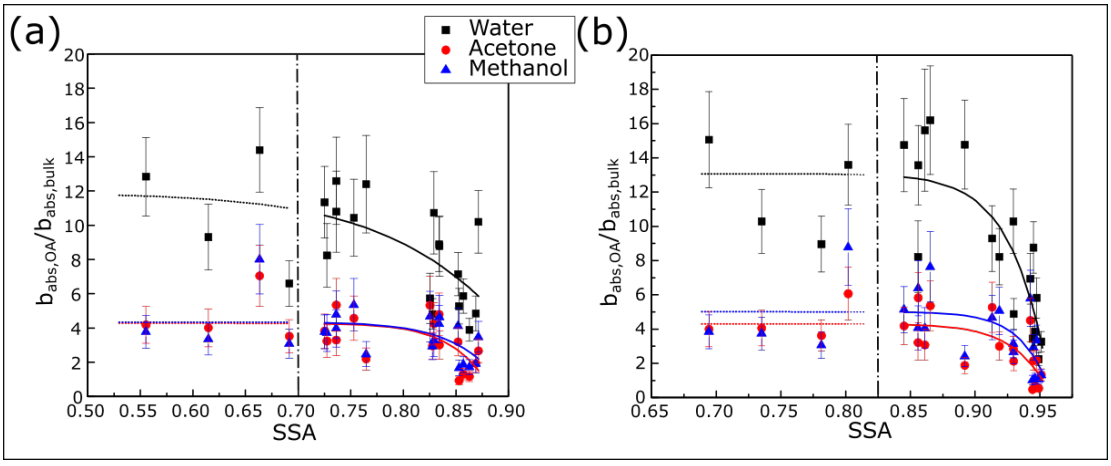

Fig. 2: Variation in $b_{abs,OA}/b_{abs,bulk}$ with change in the SSA at (a) 375 nm and (b) 405 nm. The error bars represent one standard deviation from the mean. The perforated lines separate points at lower SSA, which have high fluctuations with changing BC AÅE, from the data at high SSA.

Atmos. Chem. Phys. Discuss., https://doi.org/10.5194/acp-2018-1200
Manuscript under review for journal Atmos. Chem. Phys.
Discussion started: 21 November 2018

Atmospheric Chemistry and Physics Discussions

489

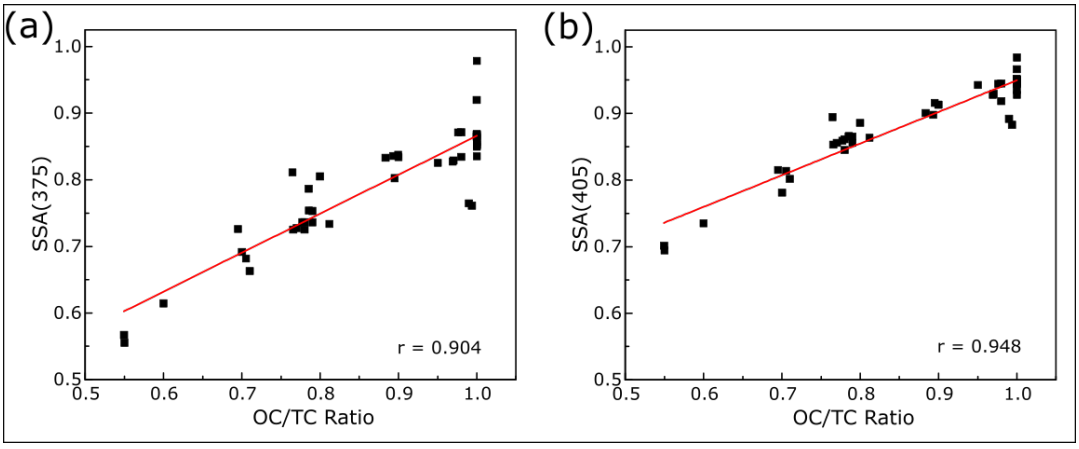

490

491 **Fig. 3:** SSA at (a) 375 nm and (b) 405 nm as a function of the OC/TC ratio. The solid red lines
492 are linear fits to the data. Pearson's r values are given at the bottom right in each plot, and the
493 parameters for the fits are listed in Table 2.

494

Atmos. Chem. Phys. Discuss., https://doi.org/10.5194/acp-2018-1200
Manuscript under review for journal Atmos. Chem. Phys.
Discussion started: 21 November 2018

Atmospheric Chemistry and Physics Discussions

495

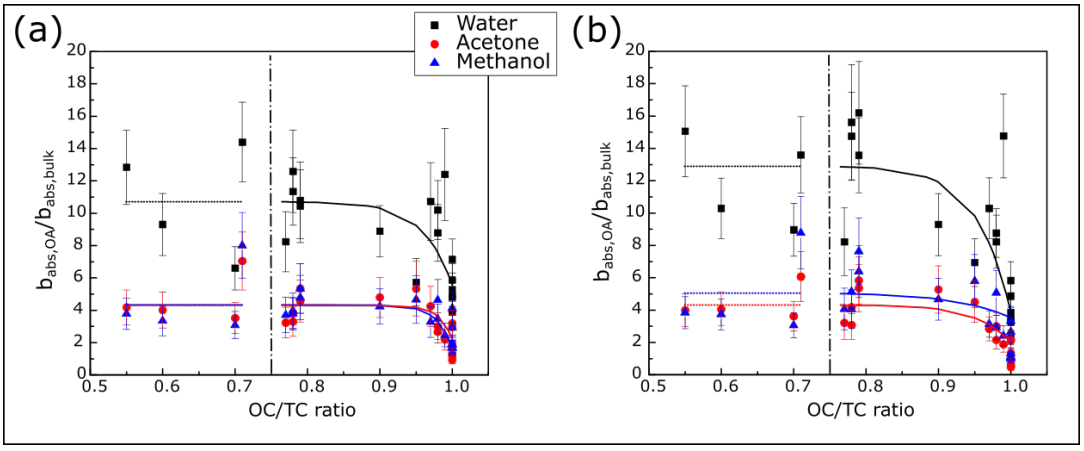

496

497 **Fig. 4:** The values of $b_{abs,OA}/b_{abs,bulk}$ plotted with the OC/TC ratio, instead of the SSA, as in Fig.

498 2.

Atmos. Chem. Phys. Discuss., https://doi.org/10.5194/acp-2018-1200
Manuscript under review for journal Atmos. Chem. Phys.
Discussion started: 21 November 2018

Atmospheric Chemistry and Physics Discussions

499 **Table 1:** Fit coefficients for $b_{abs,OA}(\lambda)/b_{abs,bulk}(\lambda)$ as a function of SSA ($y = k0 + k1\,(SSA)^{k_2}$)

500 for tested solvents and the fuels analyzed in this study along with the RMSE value for each fit.

	Wavelength (nm)	Solvent	Fit Parameters k_0	k_1	k_2	RMSE
$\frac{b_{abs,OA}}{b_{abs,bulk}}$	375	Water	11.84	-19.09	8.43	2.27
		Acetone	4.28	-50.8	24.52	1.25
		Methanol	4.34	-41.01	21.41	2.15
	405	Water	13.07	-52.3	33.34	2.46
		Acetone	4.32	-18.69	35.19	1.17
		Methanol	5.00	-29.47	42.97	1.63

501

Atmos. Chem. Phys. Discuss., https://doi.org/10.5194/acp-2018-1200
Manuscript under review for journal Atmos. Chem. Phys.
Discussion started: 21 November 2018

Table 2. Fit coefficients along with 95% confidence intervals in brackets for plots of SSA v/s OC/TC ratios (y = m (OC/TC) + c) for the different biomass fuels used in this study, and parameters for fits from Pokhrel et al. (2016) for 405 nm, along with the Pearson's r value for each linear fit.

	Wavelength (nm)	m	c	r
This study	375	0.585 (±0.040)	0.281 (±0.036)	0.904
	405	0.475 (± 0.023)	0.475 (± 0.021)	0.948
Pokhrel	405	0.874 (±0.049)	0.036 (±0.042)	0.971

Atmos. Chem. Phys. Discuss., https://doi.org/10.5194/acp-2018-1200
Manuscript under review for journal Atmos. Chem. Phys.
Discussion started: 21 November 2018

Atmospheric Chemistry and Physics Discussions

507 **Table 3:** Fit parameters for ratios of the absorption coefficient of organics in the particle phase to
508 the absorption coefficient of the bulk phase, as a function of the OC/TC ratio ($y = k_0 +$
509 $k_1(OC/TC)^{k_2}$) for the fuels analyzed in this study, along with the RMSE value for each fit.

	Wavelength (nm)	Solvent	Fit Parameters			
			k_0	k_1	k_2	RMSE
$\frac{b_{abs,OA}}{b_{abs,bulk}}$	375	Water	10.71	-5.13	24.32	2.11
		Acetone	4.26	-2.6	48.11	1.03
		Methanol	4.26	-2	53.6	2.14
	405	Water	12.89	-9.02	21.06	2.34
		Acetone	4.29	-3.28	31.5	0.97
		Methanol	4.96	-3.39	40.85	1.51

510

Atmos. Chem. Phys. Discuss., https://doi.org/10.5194/acp-2018-1200
Manuscript under review for journal Atmos. Chem. Phys.
Discussion started: 21 November 2018

Atmospheric Chemistry and Physics Discussions

511 **Table 4:** The AÅE of OA from various fuels extracted in water, acetone, and methanol, along
512 with the AÅE calculated for $b_{abs,OA}$.

Fuel	OC/TC ratio	$AÅE_{375-405}$			
		OA	Water	Acetone	Methanol
Dung	1	13.13	8.00	5.29	5.21
	1	14.44	8.95	5.85	7.75
	1	14.61	7.48	4.62	4.5
	1	14.08	8.55	5.25	6.8
Sage	1	13.53	10.87	8.62	8.8
	1	10.54	10.71	6.29	7.3
	0.97	10.41	9.88	5.2	5.8
	0.79	6.57	12.28	8.62	9.17
	0.79	7.6	10.58	8.73	8.3
	0.71	8.23	7.5	6.29	6.4
	0.55	4.4	6.48	3.84	3.6
Grass	0.99	9.8	12.08	7.84	7.5
	0.78	9.35	10.15	8.47	9.6
	0.78	6.3	9.7	7.49	7.3
	0.77	8.22	8.21	8.12	8.4
Pine	0.98	11.35	9.36	8.55	8.1
	0.98	8.43	9.59	8.36	8.6
	0.95	13.97	16.44	11.81	12.8
	0.9	7.51	9.09	8.75	8.7
	0.7	5.96	9.93	6.33	5.83
	0.6	5.04	6.36	5.2	5.4

513

Atmos. Chem. Phys. Discuss., https://doi.org/10.5194/acp-2018-1200
Manuscript under review for journal Atmos. Chem. Phys.
Discussion started: 21 November 2018

514 **Table 5:** Correction factors for bulk solution absorption to particle phase absorption, based on
515 Mie Theory calculations.

Fuel	Geometric mean (in nm)	Geometric standard deviation	Mie based Correction Factor	
			375 nm	405 nm
Sage	397	1.3	2.04 ± 0.38	2.27 ± 0.41
	271	1.32	2.05 ± 0.38	2.29 ± 0.41
	159	1.59	1.99 ± 0.36	2.15 ± 0.39

516